Voronoi-Based Coverage Control of Heterogeneous Disk-Shaped Robots

Omur Arslan and Daniel E. Koditschek

Abstract— In distributed mobile sensing applications, networks of agents that are heterogeneous respecting both actuation as well as body and sensory footprint are often modelled by recourse to power diagrams — generalized Voronoi diagrams with additive weights. In this paper we adapt the body power diagram to introduce its "free subdiagram," generating a vector field planner that solves the combined sensory coverage and collision avoidance problem via continuous evaluation of an associated constrained optimization problem. We propose practical extensions (a heuristic congestion manager that speeds convergence and a lift of the point particle controller to the more practical differential drive kinematics) that maintain the convergence and collision guarantees.

I. INTRODUCTION

Among the many proposed multiple mobile sensor coordination strategies [1], Voronoi-based coverage control [2] uniquely combines both deployment and allocation in an intrinsically distributed manner [3] via gradient descent (the "move-to-centroid" law) down a utility function minimizing the expected event sensing cost to adaptively achieve a *centroidal Voronoi configuration* (depicted on the left in Fig. 1). Since the original application to homogeneous point robots [2], a growing literature considers the extension to heterogeneous groups of robots differing variously in their sensorimotor capabilities [4]–[7] by recourse to *power diagrams* — generalized Voronoi diagrams with additive weights [8].

A. Motivation and Prior Literature

Although it inherits many nice properties of a standard Voronoi diagram such as convexity and dual triangulability, a power diagram may possibly have empty cells associated with some (unassigned) robots and/or some robots may not be contained in their nonempty cells [8], as situation depicted on the middle in Fig. 1. Such *occupancy defects* (Definition 1) generally cost resource inefficiency or redundancy[1], and, crucially, they re-introduce the problem of collision avoidance — the chief motivation for the present paper.

Voronoi-based coverage control implicitly entails collision avoidance for point robots since robots move in their pairwise disjoint Voronoi cells [2], but an additional collision avoidance strategy is mandatory for safe navigation of finite size robots. Existing work on combining coverage control and collision avoidance generally uses (i) either heuristic

[1]Note that a power diagram with an occupancy defect can be beneficial in certain applications to save/balance energy across a mobile network of power limited agents [7].
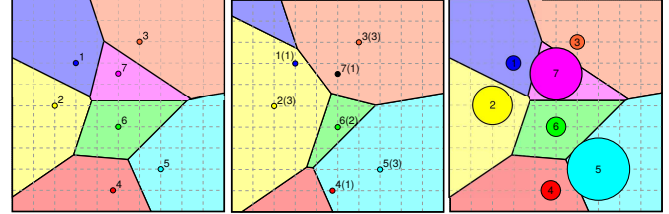

Fig. 1. An illustration of (left) the Voronoi and (middle) power diagrams of an environment based on a noncolliding placement of point robots, where the weights of power cells are shown in parentheses. Although each point robot is always contained in its Voronoi cell, power cells associated with some robots (e.g. the 7th robot) may be empty and/or some robots (e.g. the 1st and 4th robots) may not be contained in their nonempty power cells. (Right) A collision free disk configuration does not necessarily have Voronoi cells containing respective robot bodies.

approaches based on repulsive fields [9], [10] and reciprocal velocity obstacles [11] causing robots to converge to configurations far from optimal sensing configurations; or (ii) the projection of a vector field whenever a robot reaches the boundary of its partition cell [4], [12] introducing a source of discontinuity. An important observation made in [4] is that it is sufficient to restrict robot bodies to respective Voronoi regions for collision avoidance, but this is a conservative assumption for robot groups with different body sizes (as illustrated on the right in Fig. 1).

B. Contributions and Organization of the Paper

In this paper, we provide a necessary and sufficient condition for identifying collision free configurations of finite size robots in terms of their power diagrams, and accordingly propose a constrained coverage control ("move-to-constrained-centroid") law whose continuous and piecewise smooth flow asymptotically converges to an optimal sensing configuration avoiding any collisions along the way. We extend the practicability of the result by adding a congestion management heuristic for unassigned robots that hastens the assigned robots' progress, and, finally, adapt the fully actuated point particle vector field planner to the widely used kinematic differential drive vehicle model (retaining the convergence and collision avoidance guarantees in both extensions).

This paper is organized as follows. Section II briefly summarizes coverage control of point robots. Section III discusses occupancy defects of power diagrams. In Section IV we introduce a novel use of power diagrams for identifying collision free multirobot configurations, and then propose a constrained optimization framework combining area coverage and collision avoidance, and present its practical extensions. Section V offers some numerical studies of the

proposed algorithms. Section VI concludes with a summary of our contributions and a brief discussion of future work.

II. COVERAGE CONTROL OF POINT ROBOTS

A. Location Optimization of Homogeneous Robots

Let Q be a convex environment in $\mathbb{R}^N$ with a priori known event distribution function $\phi : Q \to \mathbb{R}_{>0}$ that models the probability of some event occurs in Q, and $\mathbf{p} := (\mathrm{p}_1, \mathrm{p}_2, \ldots, \mathrm{p}_n) \in Q^n$ be a (noncolliding) placement of $n \in \mathbb{N}$ point robots in Q.[2] Suppose that the event detection (sensing) cost of ith robot at location $q \in Q$ is a nondecreasing differentiable function, $f : \mathbb{R} \to \mathbb{R}$, of the Euclidean distance, $\|\mathrm{q} - \mathrm{p}_i\|$, between q and p_i. Further assume that robots are assigned to events based on a partition of Q yielding a cover, $\mathcal{W} := \{W_1, W_2, \ldots, W_n\}$, a collection of subsets ("cells"), W_i, whose union returns Q but whose cells have mutually disjoint interiors. [3] A well established approach (arising in both facility location [3], [13] and quantization [14], [15] problems) achieves such a cover by minimizing the expected event sensing cost,

$$\mathcal{H}(\mathbf{p}, \mathcal{W}) := \sum_{i=1}^{n} \int_{W_i} f(\|\mathrm{q} - \mathrm{p}_i\|) \phi(\mathrm{q}) \, \mathrm{dq}. \quad (1)$$

Now observe that, for any fixed $\mathbf{p}$, the optimal task assignment minimizing $\mathcal{H}$ is the standard Voronoi diagram $\mathcal{V}(\mathbf{p}) := \{V_1, \ldots, V_n\}$ of Q based on the configuration $\mathbf{p}$,

$$V_i = \left\{ \mathrm{q} \in Q \ \middle| \ \|\mathrm{q} - \mathrm{p}_i\| \le \|\mathrm{q} - \mathrm{p}_j\|, \forall j \ne i \right\}. \quad (2)$$

Thus, given the optimal task assignment of robots, the objective function $\mathcal{H}$ takes the following form

$$\mathcal{H}_{\mathcal{V}}(\mathbf{p}) := \mathcal{H}(\mathbf{p}, \mathcal{V}(\mathbf{p})) = \sum_{i=1}^{n} \int_{\mathcal{V}_i} f(\|\mathrm{q} - \mathrm{p}_i\|) \phi(\mathrm{q}) \, \mathrm{dq}, \quad (3)$$

and it is common knowledge that [2], [3], [15]

$$\frac{\partial \mathcal{H}_{\mathcal{V}}(\mathbf{p})}{\partial \mathrm{p}_i} = \int_{V_i} \frac{\partial}{\partial \mathrm{p}_i} f(\|\mathrm{q} - \mathrm{p}_i\|) \phi(\mathrm{q}) \, \mathrm{dq}. \quad (4)$$

In the special case of $f(x) = x^2$, the partial derivative of $\mathcal{H}_{\mathcal{V}}$ has a simple physical interpretation as follows:

$$\frac{\partial \mathcal{H}_{\mathcal{V}}(\mathbf{p})}{\partial \mathrm{p}_i} = 2m_{V_i}(\mathrm{p}_i - \mathrm{c}_{V_i}), \quad (5)$$

where m_{V_i} and c_{V_i}, respectively, denote the mass and the center of mass of V_i according to the mass density function ϕ,

$$m_{V_i} := \int_{V_i} \phi(q) \, \mathrm{d}q, \qquad \mathrm{c}_{V_i} := \int_{V_i} q \, \phi(q) \, \mathrm{d}q. \quad (6)$$

Assuming first order (completely actuated single integrator) robot dynamics,

$$\dot{\mathrm{p}}_i = \mathrm{u}_i, \quad (7)$$

the standard "move-to-centroid" law asymptotically steering point robots to a centroidal Voronoi configuration with the guarantee of no collision along the way is

$$\mathrm{u}_i = -k(\mathrm{p}_i - \mathrm{c}_{V_i}), \quad (8)$$

where $k \in \mathbb{R}_{>0}$ is a fixed control gain and the Voronoi diagram $\mathcal{V}(\mathbf{p})$ of Q is assumed to be continuously updated. Note that m_{V_i} and c_{V_i} are both continuously differentiable functions of $\mathbf{p}$ as are both $\mathcal{H}_{\mathcal{V}}$ and u_i [16]. Finally, observe, again, that the coverage control u_i supports a distributed implementation whose local communications structure is specified by the associated Delaunay graph [2].

B. Location Optimization of Heterogeneous Robots

In distributed sensing applications, heterogeneity of robotic networks in sensing and actuation [4]–[7] is often modelled by recourse to *power diagrams*, generalized Voronoi diagrams with additive weights [8]. More precisely, for a given multirobot configuration $\mathbf{p} \in Q^n$, the event sensing cost of ith robot at location $\mathrm{q} \in Q$ is assumed to be given by the *power distance*, $\|\mathrm{q} - \mathrm{p}_i\|^2 - \rho_i^2$ where $\rho_i \in \mathbb{R}_{\ge 0}$ is the *power radius* of ith robot. Accordingly, the task assignment of robots are determined by the power diagram $\mathcal{P}(\mathbf{p}, \boldsymbol{\rho}) := \{P_1, P_2, \ldots, P_n\}$ of Q based on the configuration $\mathbf{p}$ and the associated power radii $\boldsymbol{\rho} := (\rho_1, \rho_2, \ldots, \rho_n)$,

$$P_i := \left\{ \mathrm{q} \in Q \ \middle| \ \|\mathrm{q} - \mathrm{p}_i\|^2 - \rho_i^2 \le \|\mathrm{q} - \mathrm{p}_j\|^2 - \rho_j^2, \forall j \ne i \right\}, (9)$$

and the location optimization function becomes

$$\mathcal{H}_{\mathcal{P}}(\mathbf{p}, \boldsymbol{\rho}) = \sum_{i=1}^{n} \int_{P_i} \left(\|\mathrm{q} - \mathrm{p}_i\|^2 - \rho_i^2 \right) \phi(\mathrm{q}) \, \mathrm{dq}. \quad (10)$$

Note that in the special case of $\rho_i = \rho_j$ for all $i \ne j$ the power diagram $\mathcal{P}(\mathbf{p}, \boldsymbol{\rho})$ and the Voronoi diagram $\mathcal{V}(\mathbf{p})$ of Q are identical, i.e. $P_i = V_i$.

Similar to (5), for fixed $\boldsymbol{\rho}$, the partial derivative of $\mathcal{H}_{\mathcal{P}}$ takes the following simple form [4], [7], [10],

$$\frac{\partial \mathcal{H}_{\mathcal{P}}(\mathbf{p}, \boldsymbol{\rho})}{\partial \mathrm{p}_i} = 2m_{P_i}(\mathrm{p}_i - \mathrm{c}_{P_i}), \quad (11)$$

where m_{P_i} and c_{P_i} are the mass and the center of mass of P_i, respectively, as defined in (6). [4] For the single integrator robot model (7), the standard "move-to-centroid" law of heterogeneous robotic networks asymptotically driving robots to a critical point of $\mathcal{H}_{\mathcal{P}}(., \boldsymbol{\rho})$, where robots are located at the centroids of their respective power cells, is defined as

$$\mathrm{u}_i = -k(\mathrm{p}_i - \mathrm{c}_{P_i}), \quad (12)$$

for some fixed $k \in \mathbb{R}_{>0}$ and the power diagram $\mathcal{P}(\mathbf{p}, \boldsymbol{\rho})$ of Q is assumed to be continuously updated. Notwithstanding its welcome inheritance of many standard Voronoi properties (e.g., convexity, dual triangulability), a power diagram may yield empty cells associated with some robots and/or some robots may not be contained in their nonempty power cells, illustrated in Fig. 1. In consequence, contrary to the case

---

[2] Here, $\mathbb{N}$ is the set of all natural numbers; $\mathbb{R}$ and $\mathbb{R}_{>0}$ ($\mathbb{R}_{\ge 0}$) denote the set of real and positive (nonnegative) real numbers, respectively; and $\mathbb{R}^N$ is the N-dimensional Euclidean space.

[3] We will generally refer to such decompositions as "diagrams" but also occasionally allow the slight abuse of language to follow tradition and refer to $\mathcal{W}$ as a *partition*.

[4] To be well defined we set $\mathrm{c}_{P_i} = \mathrm{p}_i$ whenever P_i has an empty interior.

of homogeneous robots, the "move-to-centroid" law of heterogeneous point robots is discontinuous and it cannot guarantee collision free navigation. Thus, in past literature, for robots of finite but heterogeneous size, the standard "move-to-centroid" law inevitably requires an additional heuristic collision avoidance strategy for safe navigation.

III. OCCUPANCY DEFECTS OF POWER DIAGRAMS

Definition 1 (*Occupancy Defect*) The *power partition*, $\mathcal{P}(\mathbf{p}, \boldsymbol{\rho})$, associated with configuration $\mathbf{p} \in Q^n$ and radii $\boldsymbol{\rho} \in (\mathbb{R}_{\geq 0})^n$ is said to have an *occupancy defect* if $\mathrm{p}_i \notin P_i$ for some $i \in \{1, 2, \ldots n\}$.

Configurations incurring occupancy defects introduce a number of problems. First of all, empty partition cells cause resource redundancy because some robots may never be assigned to any event happening around them. Such robots do not only become redundant, but also complicate collision avoidance as (moving or stationary) obstacles and limit the mobility of others. In general, robots that are not contained in their respective cells require an extra care for collision avoidance.

A straightforward characterization of an occupancy defective configuration is: [5]

Proposition 1 *Given radii $\boldsymbol{\rho} \in (\mathbb{R}_{\geq 0})^n$, configuration $\mathbf{p} \in Q^n$ does not incur an occupancy defective power diagram if and only if $\|\mathrm{p}_i - \mathrm{p}_j\|^2 \geq |\rho_i^2 - \rho_j^2|$ for all $i \neq j$.*

Proof. By Definition 1, $\mathcal{P}(\mathbf{p}, \boldsymbol{\rho})$ has no occupancy defect if and only if $\mathrm{p}_i \in P_i$ for all i, which is the case if and only if

$$\|\mathrm{p}_i - \mathrm{p}_i\|^2 - \rho_i^2 \leq \|\mathrm{p}_i - \mathrm{p}_j\|^2 - \rho_j^2, \quad (13)$$

$$\|\mathrm{p}_j - \mathrm{p}_j\|^2 - \rho_j^2 \leq \|\mathrm{p}_j - \mathrm{p}_i\|^2 - \rho_i^2, \quad (14)$$

for all $i \neq j$. Thus, the result follows. ∎

IV. COMBINING COVERAGE CONTROL AND COLLISION AVOIDANCE

Throughout the rest of paper, we consider heterogeneous disk-shaped multirobot configurations, $\mathbf{p} = (\mathrm{p}_1, \mathrm{p}_2, \ldots, \mathrm{p}_n) \in Q^n$, in Q with associated vectors of nonnegative body radii $\boldsymbol{\beta} := (\beta_1, \beta_2, \ldots, \beta_n) \in (\mathbb{R}_{\geq 0})^n$ and sensory footprint radii $\boldsymbol{\sigma} := (\sigma_1, \sigma_2, \ldots, \sigma_n) \in (\mathbb{R}_{\geq 0})^n$, where ith robot is centered at $\mathrm{p}_i \in Q$ and has body radius $\beta_i \geq 0$ and sensory footprint radius $\sigma_i \geq 0$. Accordingly, we will denote by $\mathcal{B}(\mathbf{p}, \boldsymbol{\beta}) = \{B_1, B_2, \ldots, B_n\}$, a cover we term the *body diagram* of Q, solving the power problem (9), (10), defined from $\mathcal{H}_{\mathcal{B}}(\mathbf{p}, \boldsymbol{\beta})$; and we will denote by $\mathcal{S}(\mathbf{p}, \boldsymbol{\sigma}) = \{S_1, S_2, \ldots, S_n\}$, a cover we term the *sensor diagram* of Q, solving the corresponding problem defined by $\mathcal{H}_{\mathcal{S}}(\mathbf{p}, \boldsymbol{\sigma})$. We also find it convenient to denote the configuration space of body-noncolliding disks of radii $\boldsymbol{\beta}$ in Q as

$$\mathrm{Conf}(Q, \boldsymbol{\beta}) := \Big\{ \mathbf{p} \in Q^n \Big| \|\mathrm{p}_i - \mathrm{p}_j\| > \beta_i + \beta_j \ \ \forall i \neq j,$$
$$D(\mathrm{p}_i, \beta_i) \subset \mathring{Q} \ \ \forall i \Big\}, \quad (15)$$

where $D(\mathrm{x}, r) := \{\mathrm{y} \in \mathbb{R}^N \,|\, \|\mathrm{x} - \mathrm{y}\| \leq r\}$ is the closed disk in $\mathbb{R}^N$ centered at $\mathrm{x} \in \mathbb{R}^N$ with radius $r \geq 0$, and $\mathring{Q}$ is the interior of Q. Note that the vectors of body radii $\boldsymbol{\beta}$ and sensory footprint radii $\boldsymbol{\sigma}$ are not necessary equal since $\boldsymbol{\beta}$ models the heterogeneity of robots in body size, $\boldsymbol{\sigma}$ models their heterogeneity in sensing and actuation.

A. Encoding Collisions via Body Diagrams

A geometric characterization of collision free multirobot configurations in Q via their body diagrams is:

Proposition 2 *Let $\mathcal{B}(\mathbf{p}, \boldsymbol{\beta})$ be the body diagram of Q associated with configuration $\mathbf{p} \in Q^n$ and body radii $\boldsymbol{\beta} \in (\mathbb{R}_{\geq 0})^n$. Then $\mathbf{p}$ is collision free if and only if every robot body is contained in the interior of its body cell, i.e.*

$$\mathbf{p} \in \mathrm{Conf}(Q, \boldsymbol{\beta}) \iff D(\mathrm{p}_i, \beta_i) \subset \mathring{B}_i \ \ \forall i. \quad (16)$$

Proof. The sufficiency ($\Longleftarrow$) follows because $\mathcal{B}(\mathbf{p}, \boldsymbol{\beta})$ is a cover of Q whose elements have disjoint interiors. Hence, given $D(\mathrm{p}_i, \beta_i) \subset \mathring{B}_i$ for all i, we have $D(\mathrm{p}_i, \beta_i) \subset \mathring{Q}$ and $D(\mathrm{p}_i, \beta_i) \cap D(\mathrm{p}_j, \beta_j) = \emptyset$ for all $i \neq j$, and so $\|\mathrm{p}_i - \mathrm{p}_j\| > \beta_i + \beta_j$. Thus, $\mathbf{p} \in \mathrm{Conf}(Q, \boldsymbol{\beta})$.

To see the necessity ($\Longrightarrow$), for any $\mathbf{p} \in \mathrm{Conf}(Q, \boldsymbol{\beta})$ we will show that $\mathrm{p}_i \in B_i$ for all i, and the distance between p_i and the boundary ∂B_i of B_i is greater than β_i, i.e. $\min_{\mathrm{x} \in \partial B_i} \|\mathrm{x} - \mathrm{p}_i\| > \beta_i$, and so $D(\mathrm{p}_i, \beta_i) \subset \mathring{B}_i$.

It follows from Proposition 1 that for any $\mathbf{p} \in \mathrm{Conf}(Q, \boldsymbol{\beta})$ $\mathcal{B}(\mathbf{p}, \boldsymbol{\beta})$ has no occupancy defect (Def. 1), i.e. $\mathrm{p}_i \in B_i \ \forall i$.

The boundary ∂B_i of B_i is defined by the boundary ∂Q of Q and the separating separating hyperplane between body cells B_i and B_j for some $j \neq i$ [8]. By definition (15), we have $\min_{\mathrm{x} \in \partial Q} \|\mathrm{x} - \mathrm{p}_i\| > \beta_i$ for any $\mathbf{p} \in \mathrm{Conf}(Q, \boldsymbol{\beta})$.

Now observe that, for any $i \neq j$ the separating hyperplane between body cells B_i and B_j is perpendicular to the line joining p_i and p_j and is given by [8]

$$H_{ij} := \Big\{ \mathrm{x} \in \mathbb{R}^N \Big| 2\mathrm{x}^{\mathrm{T}}(\mathrm{p}_i - \mathrm{p}_j) = \beta_j^2 - \beta_i^2 + \|\mathrm{p}_i\|^2 - \|\mathrm{p}_j\|^2 \Big\}, (17)$$

and the perpendicular distance of p_i to H_{ij} is given by

$$d(\mathrm{p}_i, H_{ij}) := \frac{\|\mathrm{p}_i - \mathrm{p}_j\|}{2} + \frac{\beta_i^2 - \beta_j^2}{2\|\mathrm{p}_i - \mathrm{p}_j\|}. \quad (18)$$

Note that $d(\mathrm{p}_i, H_{ij})$ is negative when $\mathcal{B}(\mathbf{p}, \boldsymbol{\beta})$ has an occupancy defect; and we have from Proposition 1 that $\mathcal{B}(\mathbf{p}, \boldsymbol{\beta})$ is free of such a defect for any $\mathbf{p} \in \mathrm{Conf}(Q, \boldsymbol{\beta})$ and so $d(\mathrm{p}_i, H_{ij}) \geq 0$. One can further show that for any $i \neq j$

$$d(\mathrm{p}_i, H_{ij}) = \beta_i + \frac{\|\mathrm{p}_i - \mathrm{p}_i\|^2 + \beta_i^2 - \beta_j^2 - 2\beta_i\|\mathrm{p}_i - \mathrm{p}_i\|}{2\|\mathrm{p}_i - \mathrm{p}_i\|},$$
$$= \beta_i + \underbrace{\frac{(\|\mathrm{p}_i - \mathrm{p}_i\| - \beta_i)^2 - \beta_j^2}{2\|\mathrm{p}_i - \mathrm{p}_i\|}}_{>0, \text{ since } \mathbf{p} \in \mathrm{Conf}(Q, \boldsymbol{\beta})} > \beta_i, \quad (19)$$

which completes the proof. ∎

To determine a collision free neighborhood of a configuration $\mathbf{p} \in \mathrm{Conf}(Q, \boldsymbol{\beta})$ with a vector of body radii $\boldsymbol{\beta} \in (\mathbb{R}_{\geq 0})^n$,
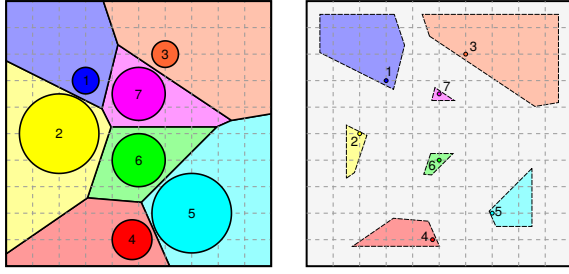
Fig. 2. (left) Encoding collision free configurations via body diagrams: A configuration of disks is nonintersecting iff each disk is contained in the interior of its body cell. (right) Free subcells, obtained by eroding each body cell with its associated disk radius.

we define a *free subdiagram* $\mathcal{F}(\mathbf{p}, \boldsymbol{\beta}) := \{F_1, F_2, \ldots, F_n\}$ of the body diagram $\mathcal{B}(\mathbf{p}, \boldsymbol{\beta}) = \{B_1, B_2, \ldots, B_n\}$ by eroding each cell removing the volume swept along its boundary, ∂B_i, by the associated body radius, see Fig. 2, as [17] [6]

$$F_i := B_i \backslash \left(\partial B_i \oplus D(\mathbf{0}, \beta_i) \right) = \left\{ q \in B_i \,\middle|\, \min_{x \in \partial B_i} \|x - q\| > \beta_i \right\}. (20)$$

Note that F_i is a nonempty convex set because $p_i \in F_i$ and the erosion of a convex set by a ball is convex. [7]

The following observation yields a (possibly conservative) convex inner approximation of the free configuration space neighborhood surrounding free configuration as

$$\mathbf{p} \in \mathrm{Conf}(Q, \boldsymbol{\beta}) \Rightarrow \prod \mathcal{F}(\mathbf{p}, \boldsymbol{\beta}) \subset \mathrm{Conf}(Q, \boldsymbol{\beta}), \quad (21)$$

where $\prod \mathcal{F}(\mathbf{p}, \boldsymbol{\beta}) = F_1 \times F_2 \times \ldots \times F_n$.

Lemma 1 *Let $\mathbf{p} \in \mathrm{Conf}(Q, \boldsymbol{\beta})$ be a multirobot configuration with a vector of body radii $\boldsymbol{\beta} \in (\mathbb{R}_{\geq 0})^n$, and $\mathcal{F}(\mathbf{p}, \boldsymbol{\beta})$ be the free subdiagram of the body diagram $\mathcal{B}(\mathbf{p}, \boldsymbol{\beta})$.*

Then $\mathbf{q} \in Q^n$ is a collision free multirobot configuration in $\mathrm{Conf}(Q, \boldsymbol{\beta})$ if $q_i \in F_i$ (i.e. $D(q_i, \beta_i) \subset \mathring{B}_i$) for all i.

Proof. The results directly follows from $\mathcal{B}(\mathbf{p}, \boldsymbol{\beta})$ covering a partition of Q, as discussed in the proof of Proposition 2. ∎

B. Coverage Control of Heterogeneous Disk-Shaped Robots

Consider a heterogeneous multirobot configuration $\mathbf{p} \in \mathrm{Conf}(Q, \boldsymbol{\beta} + \boldsymbol{\epsilon})$ with associated vectors of body radii $\boldsymbol{\beta} \in (\mathbb{R}_{\geq 0})^n$, safety margins $\boldsymbol{\epsilon} \in (\mathbb{R}_{>0})^n$ and sensory footprint radii $\boldsymbol{\sigma} \in (\mathbb{R}_{\geq 0})^n$, and let $\mathcal{S}(\mathbf{p}, \boldsymbol{\sigma}) = \{S_1, \ldots, S_n\}$ be the sensory diagram of Q based on robot locations $\mathbf{p}$ and sensory footprint radii $\boldsymbol{\sigma}$, and $\mathcal{F}(\mathbf{p}, \boldsymbol{\beta} + \boldsymbol{\epsilon}) = \{F_1, \ldots, F_n\}$ be the free subdiagram associated with configuration $\mathbf{p}$ and enlarged body radii $\boldsymbol{\beta} + \boldsymbol{\epsilon}$. Here we use $\boldsymbol{\epsilon}$ to guarantee the clearance between any pair $i \neq j$ of robots to be at least $\epsilon_i + \epsilon_j$. [8]

[6] Here, $\mathbf{0}$ is a vector of all zeros with the appropriate size, and $A \oplus B := \{a + b \mid a \in A, b \in B\}$ is the Minkowski sum of sets A and B.

[7] It is obvious that the erosion of a half-space by a ball is a half-space. Hence, since the erosion operation is distributed over set intersection [17], and a convex set can be defined as (possibly infinite) intersection of half-spaces [18], the erosion of a convex set by a ball is convex.

[8] Having a positive vector of safety margins $\boldsymbol{\epsilon}$ enables us to consider collision free configurations in $\overline{\mathrm{Conf}}(Q, \boldsymbol{\beta} + \boldsymbol{\epsilon}) \subset \mathrm{Conf}(Q, \boldsymbol{\beta})$. Throughout the rest of the paper, in order the compress the notation, we will abuse the notation and use $\mathrm{Conf}(Q, \boldsymbol{\beta} + \boldsymbol{\epsilon})$ to refer to the closure of the configuration space in (15).

Now, in contrast to the standard "move-to-centroid" law that steers each robot directly towards the centroid, c_{S_i}, of its sensory cell, S_i, we propose a coverage control policy that selects a safe target location, called the *constrained centroid* of S_i, that solves the following convex programming [9]

$$\begin{aligned} \text{minimize} \quad & \|q_i - c_{S_i}\|^2 \\ \text{subject to} \quad & q_i \in \overline{F}_i \end{aligned} \quad (22)$$

where $\overline{F}_i$ is a closed convex set. It is well known that the unique solution of (22) is given by [18, Section 8.1.1] [10]

$$\overline{c}_{S_i} := \begin{cases} c_{S_i} & , \text{ if } c_{S_i} \in \overline{F}_i, \\ \Pi_{\overline{F}_i}(c_{S_i}) & , \text{ otherwise,} \end{cases} \quad (23)$$

where $\Pi_C(x)$ denotes the metric projection of $x \in \mathbb{R}^N$ onto a convex set $C \subset \mathbb{R}^N$, and note that Π_C is piecewise continuously differentiable [20]. [11] Accordingly, for the single integrator robot dynamics (7), our "move-to-constrained-centroid" law is defined as

$$u_i = -k(p_i - \overline{c}_{S_i}), \quad (24)$$

where $k \in \mathbb{R}_{>0}$ is a fixed control gain, and we assume that $\mathcal{S}(\mathbf{p}, \boldsymbol{\sigma})$ and $\mathcal{F}(\mathbf{p}, \boldsymbol{\beta} + \boldsymbol{\epsilon})$ are continuously updated. We find it convenient to have $G_{\mathcal{S}}(Q, \boldsymbol{\beta} + \boldsymbol{\epsilon}, \boldsymbol{\sigma})$ denote the set of equilibria of our "move-to-constrained-centroid" law where robots are located at the constrained centroid of their respective sensory cells, [12]

$$G_{\mathcal{S}}(Q, \boldsymbol{\beta} + \boldsymbol{\epsilon}, \boldsymbol{\sigma}) := \left\{ \mathbf{p} \in \mathrm{Conf}(Q, \boldsymbol{\beta} + \boldsymbol{\epsilon}) \,\middle|\, p_i = \overline{c}_{S_i} \, \forall i \right\}. (25)$$

In the special case of identical sensory footprint radii, i.e. $\sigma_i = \sigma_j$ for all $i \neq j$, these stationary configurations are called the constrained centroidal Voronoi configurations [21]. Also note that for homogeneous point robots our "move-to-constrained-centroid" law in (24) simplifies back to the standard "move-to-centroid" law in (8).

We summarize the qualitative properties of our "move-to-constrained-centroid" law as follows:

Theorem 1 *For any choice of vectors of body radii $\boldsymbol{\beta} \in (\mathbb{R}_{\geq 0})^n$, safety margin $\boldsymbol{\epsilon} \in (\mathbb{R}_{>0})^n$ and sensory footprint radii $\boldsymbol{\sigma} \in (\mathbb{R}_{\geq 0})^n$, the configuration space of nonintersecting disks $\mathrm{Conf}(Q, \boldsymbol{\beta} + \boldsymbol{\epsilon})$ (15) is positive invariant under the "move-to-constrained-centroid" law in (24) whose unique, continuous and piecewise differentiable flow, starting at any configuration in $\mathrm{Conf}(Q, \boldsymbol{\beta} + \boldsymbol{\epsilon})$, asymptotically reaches a locally optimal sensing configuration in $G_{\mathcal{S}}(Q, \boldsymbol{\beta} + \boldsymbol{\epsilon}, \boldsymbol{\sigma})$ while*

[9] Here, $\overline{A}$ is the closure of set A.

[10] In general, the metric projection of a point onto a convex set can be efficiently computed using a standard convex programming solver [18]. If Q is a convex polytope, then a free subcell, F_i, is also a convex polytope and can be written as a finite intersection of half-spaces. Hence, the metric projection onto a convex polytope can be recast as quadratic programming and can be solved in polynomial time [19]. In the case of a convex polygonal environment, F_i is a convex polygon and the metric projection onto a convex polygon can be solved analytically since the solution lies on one of its edges unless the input point is inside the polygon.

[11] Note that c_{S_i} is well defined (see footnote 4), hence $\overline{c}_{S_i}$ must be as well given $F_i \neq \emptyset$.

[12] Note that this set cannot be empty since it contains the minima of a smooth function over a compact set (22).

strictly decreasing the utility function $\mathcal{H}_S(\cdot, \boldsymbol{\sigma})$ *(10) along the way. If an equilibrium in* $G_S(Q, \boldsymbol{\beta}+\boldsymbol{\epsilon}, \boldsymbol{\sigma})$ *is isolated, then it is locally asymptotically stable.*

Proof. The instantaneous "target" in (24) lies in the closure of the convex inner approximation to the freespace neighborhood of any free configuration, $\overline{c}_{S(\mathbf{p}, \boldsymbol{\sigma})} \in \prod \mathcal{F}(\mathbf{p}, \boldsymbol{\beta}+\boldsymbol{\epsilon}) \subset \text{Conf}(Q, \boldsymbol{\beta}+\boldsymbol{\epsilon})$, hence, according to Lemma 1, the configuration space tangent vector defined by (24), $-k\left(\mathbf{p} - \overline{c}_{S(\mathbf{p}, \boldsymbol{\sigma})}\right) \in T_{\mathbf{p}}\text{Conf}(Q, \boldsymbol{\beta}+\boldsymbol{\epsilon})$, is either interior directed or, at worse, tangent to the boundary of $\prod \mathcal{F}(\mathbf{p}, \boldsymbol{\beta}+\boldsymbol{\epsilon})$. Therefore, by construction (22), the "move-to-constrained-centroid" law leaves $\text{Conf}(Q, \boldsymbol{\beta}+\boldsymbol{\epsilon})$ positively invariant.

The existence, uniqueness and continuity of its flow can be observed using an equivalent hybrid system consisting of a family of piecewise continuously differentiable local vector fields as follows. Let $\mathbf{u}^I : \mathcal{D}_I \to \left(\mathbb{R}^N\right)^n$ be a local controller associated with a subset I of $\{1, 2, \ldots, n\}$ defined as

$$\mathbf{u}_i^I = \begin{cases} -k\left(\mathbf{p}_i - \overline{c}_{S_i}\right), & \text{if } i \in I \\ \mathbf{0}, & \text{otherwise,} \end{cases} \quad (26)$$

where its domain is

$$\mathcal{D}_I := \left\{ \mathbf{p} \in \text{Conf}(Q, \boldsymbol{\beta}+\boldsymbol{\epsilon}) \, \middle| \, \overset{\circ}{S}_i \neq \emptyset \quad \forall i \in I \right\}. \quad (27)$$

Note that for a given configuration in its domain, $\mathcal{D}_I$, a local policy index, I, indicates which robots are assigned to sensory cells with nonempty interiors, and so the domains, $\mathcal{D}_I$, of local controllers defines a finite open cover of $\text{Conf}(Q, \boldsymbol{\beta}+\boldsymbol{\epsilon})$. Hence, since all unassigned robots are stationary under the "move-to-constrained-centroid" law and every robot whose sensory cell has a nonempty interior is assigned to the coverage task, one can further conclude that these local controllers can be composed using the policy selection strategy, $g : \text{Conf}(Q, \boldsymbol{\beta}+\boldsymbol{\epsilon}) \to \mathbb{P}(n)$ maximizing the number of assigned robots,[13]

$$g(\mathbf{p}) := \underset{\substack{I \subseteq \{1, \ldots, n\} \\ \mathbf{p} \in \mathcal{D}_I}}{\arg \max} |I|. \quad (28)$$

such that the resulting hybrid vector field is the same as the "move-to-constrained-centroid" law in (24), i.e. for any $\mathbf{p} \in \text{Conf}(Q, \boldsymbol{\beta}+\boldsymbol{\epsilon})$

$$\mathbf{u}(\mathbf{p}) = \mathbf{u}^{g(\mathbf{p})}(\mathbf{p}). \quad (29)$$

Note that, since a sensory cell with a nonempty interior can not instantaneously appear or disappear under any continuous motion, each time when a local controller is selected by g it steers the robots for a nonzero time.

Now the continuity properties of each local control policy can be observed as follows. As in the case of Voronoi diagrams [16], we have that the boundary of a sensory cell with a nonempty interior is a piecewise continuously differentiable function of robot locations, and its centroid is continuously differentiable with respect to robot locations. Similarly, the boundary of each element of $\mathcal{F}(\mathbf{p}, \boldsymbol{\beta}+\boldsymbol{\epsilon})$ is

piecewise continuously differentiable since each free cell is a nonempty erosion of an element of the body diagram $\mathcal{B}(\mathbf{p}, \boldsymbol{\beta}+\boldsymbol{\epsilon})$ by a fixed closed ball. Hence, one can conclude that each local control policy is piecewise continuously differentiable since metric projections onto convex cells are piecewise continuously differentiable [20] and the composition of piecewise continuously differentiable functions are also piecewise continuously differentiable [22].

Therefore, the existence, uniqueness and continuously differentiability of the flow of each local controller $\mathbf{u}^I$ follow from the Lipschitz continuity of $\mathbf{u}^I$ in its compact domain $\mathcal{D}_I$ since a piecewise continuously differentiable function is also locally Lipschitz on its domain [22] and a locally Lipschitz function on a compact set is globally Lipschitz on that set [23]. Hence, since their domains define a finite open cover of $\text{Conf}(Q, \boldsymbol{\beta}+\boldsymbol{\epsilon})$, the unique, continuous and piecewise differentiable flow of the "move-to-constrained-centroid" law is constructed by piecing together trajectories of these local policies.

Finally, a natural choice of a Lyapunov function for the stability analysis is the continuously differentiable location optimization function $\mathcal{H}_S$ (10), and one can verify from (11), (22) and (24) that for any $\mathbf{p} \in \text{Conf}(Q, \boldsymbol{\beta}+\boldsymbol{\epsilon})$ [14]

$$\dot{\mathcal{H}}_S(\mathbf{p}, \boldsymbol{\sigma}) = -k \sum_{i=1}^{n} m_{S_i} \underbrace{2(\mathbf{p}_i - c_{S_i})^{\mathrm{T}}(\mathbf{p}_i - \overline{c}_{S_i})}_{\substack{\geq \|\mathbf{p}_i - \overline{c}_{S_i}\|^2, \\ \text{since } \mathbf{p}_i \in F_i \text{ and } \|\mathbf{p}_i - c_{S_i}\|^2 \geq \|\overline{c}_{S_i} - c_{S_i}\|^2}}, \quad (30)$$

$$\leq -k \sum_{i=1}^{n} m_{S_i} \|\mathbf{p}_i - \overline{c}_{S_i}\|^2 \leq 0, \quad (31)$$

which is equal to 0 only if $\mathbf{p}_i = \overline{c}_{S_i}$ for all i, i.e. $\mathbf{p} \in G_S(Q, \boldsymbol{\beta}+\boldsymbol{\epsilon}, \boldsymbol{\sigma})$. Thus, it follows from LaSalle's Invariance Principle [23] that all multirobot configurations in $\text{Conf}(Q, \boldsymbol{\beta}+\boldsymbol{\epsilon})$ asymptotically reach $G_S(Q, \boldsymbol{\beta}+\boldsymbol{\epsilon}, \boldsymbol{\sigma})$. If an equilibrium $\mathbf{p}^*$ in $G_S(Q, \boldsymbol{\beta}+\boldsymbol{\epsilon}, \boldsymbol{\sigma})$ is isolated, then it is guaranteed that $\dot{\mathcal{H}}_S(\mathbf{p}, \boldsymbol{\sigma}) < 0$ in a neighborhood of $\mathbf{p}^*$, and so it is locally asymptotically stable [24]. ∎

C. Congestion Control of Unassigned Robots

In this subsection we shall present a heuristic congestion management strategy for unassigned robots that improves assigned robots' progress.

For a choice of vectors of body radii $\boldsymbol{\beta} \in (\mathbb{R}_{\geq 0})^n$, safety margins $\boldsymbol{\epsilon} \in (\mathbb{R}_{>0})^n$ and sensory footprint radii $\boldsymbol{\sigma} \in (\mathbb{R}_{\geq 0})^n$, let $\mathbf{p} \in \text{Conf}(Q, \boldsymbol{\beta}+\boldsymbol{\epsilon})$ be a multirobot configuration in Q with the associated body diagram $\mathcal{B}(\mathbf{p}, \boldsymbol{\beta}+\boldsymbol{\epsilon}) = \{B_1, \ldots, B_n\}$, free subdiagram $\mathcal{F}(\mathbf{p}, \boldsymbol{\beta}+\boldsymbol{\epsilon}) = \{F_1, \ldots, F_n\}$ and sensory diagram $S(\mathbf{p}, \boldsymbol{\sigma}) = \{S_1, \ldots, S_n\}$.

Consider the following heuristic management of robots: if ith robot has a sensory cell P_i with a nonempty interior, then it is assigned to the coverage task with sensory cell S_i; otherwise, since the robot becomes redundant for the coverage task, it is assigned to move towards a safe location

---

[13]Here $\mathbb{P}(n)$ denotes the set of all subsets of $\{1, 2, \ldots, n\}$.

[14]$\mathbf{A}^{\mathrm{T}}$ is the transpose of matrix $\mathbf{A}$.

in B_i. We therefore define the set of *"active"* domains $\mathcal{A}\left(\mathbf{p}, \boldsymbol{\beta}+\boldsymbol{\epsilon}, \boldsymbol{\sigma}\right) = \{A_1, A_2, \ldots, A_n\}$ of robots as

$$A_i := \begin{cases} S_i & , \text{ if } \mathring{S}_i \neq \emptyset, \\ B_i & , \text{ otherwise.} \end{cases} \quad (32)$$

Note that $\mathcal{A}\left(\mathbf{p}, \boldsymbol{\beta}+\boldsymbol{\epsilon}, \boldsymbol{\sigma}\right)$ defines a cover of Q and its elements have nonempty interior for all $\mathbf{p} \in \mathrm{Conf}\left(Q, \boldsymbol{\beta}+\boldsymbol{\epsilon}\right)$ (Proposition 2).

For the first order robot dynamics (7), we propose the following "move-to-constrained-active-centroid" law

$$\mathrm{u}_i = -k\left(\mathrm{p}_i - \overline{\mathrm{c}}_{A_i}\right), \quad (33)$$

that steers each robot towards the constrained centroid, $\overline{\mathrm{c}}_{A_i}$ as defined in (23), of its active domain, A_i, which is the closest point in $\overline{F}_i$ to the centroid c_{A_i} and so uniquely solves [18]

$$\begin{aligned} \text{minimize} \quad & \|\mathrm{q}_i - \mathrm{c}_{A_i}\|^2 \\ \text{subject to} \quad & \mathrm{q}_i \in \overline{F}_i \end{aligned} \quad (34)$$

where $\overline{F}_i$ is convex and $k \in \mathbb{R}_{>0}$ is a fixed control gain. Once again, we assume that $\mathcal{A}\left(\mathbf{p}, \boldsymbol{\beta}+\boldsymbol{\epsilon}, \boldsymbol{\sigma}\right)$ and $\mathcal{F}\left(\mathbf{p}, \boldsymbol{\beta}+\boldsymbol{\epsilon}\right)$ are continuously updated. It is also useful to have $G_{\mathcal{A}}\left(Q, \boldsymbol{\beta}+\boldsymbol{\epsilon}, \boldsymbol{\sigma}\right)$ denote the set of equilibria of the "move-to-constrained-active-centroid" law where robots are located at the constrained centroid of their active domains,

$$G_{\mathcal{A}}(Q, \boldsymbol{\beta}+\boldsymbol{\epsilon}, \boldsymbol{\sigma}) := \left\{ \mathbf{p} \in \mathrm{Conf}\left(Q, \boldsymbol{\beta}+\boldsymbol{\epsilon}\right) \middle| \mathrm{p}_i = \overline{\mathrm{c}}_{A_i} \; \forall i \right\}. (35)$$

We summarize some important properties of our "move-to-constrained-active-centroid" law as follows:

Proposition 3 *For any* $\boldsymbol{\beta}, \boldsymbol{\sigma} \in \left(\mathbb{R}_{\geq 0}\right)^n$ *and* $\boldsymbol{\epsilon} \in \left(\mathbb{R}_{>0}\right)^n$, *the "move-to-constrained-active-centroid" law in (33) leaves the configuration space of nonintersecting disks* $\mathrm{Conf}(Q, \boldsymbol{\beta}+\boldsymbol{\epsilon})$ *positively invariant; and its unique, continuous and piecewise differentiable flow, starting at any configuration in* $\mathrm{Conf}(Q, \boldsymbol{\beta}+\boldsymbol{\epsilon})$, *asymptotically reaches* $G_{\mathcal{A}}(Q, \boldsymbol{\beta}+\boldsymbol{\epsilon}, \boldsymbol{\sigma})$ *without increasing the utility function* $\mathcal{H}_{\mathbb{S}}(\cdot, \boldsymbol{\sigma})$ *(10) along the way.*

Proof. The positive invariance of $\mathrm{Conf}\left(Q, \boldsymbol{\beta}+\boldsymbol{\epsilon}\right)$ under the "move-to-constrained-active-centroid" law and the existence, uniqueness and continuity properties of its flow follow the same pattern as established in Theorem 1.

For the stability analysis, using (11), (33) and (34), one can show that the continuously differentiable utility function $\mathcal{H}_{\mathbb{S}}(., \boldsymbol{\sigma})$ (10) is nonincreasing along the trajectory of the "move-to-constrained-active-centroid" law as follows:

$$\dot{\mathcal{H}}_{\mathbb{S}}\left(\mathbf{p}, \boldsymbol{\sigma}\right) = -k \sum_{\substack{i \in \{1, \ldots, n\} \\ \mathring{S}_i \neq \emptyset}} m_{S_i} \underbrace{2(\mathrm{p}_i - \mathrm{c}_{S_i})^{\mathrm{T}}(\mathrm{p}_i - \overline{\mathrm{c}}_{S_i})}_{\substack{\geq \|\mathrm{p}_i - \overline{\mathrm{c}}_{S_i}\|^2, \\ \text{since } \mathrm{p}_i \in F_i \text{ and } \|\mathrm{p}_i - \mathrm{c}_{S_i}\|^2 \geq \|\overline{\mathrm{c}}_{S_i} - \mathrm{c}_{S_i}\|^2}}$$
$$- k \sum_{\substack{i \in \{1, \ldots, n\} \\ \mathring{S}_i = \emptyset}} m_{S_i} \underbrace{2(\mathrm{p}_i - \mathrm{c}_{S_i})^{\mathrm{T}}(\mathrm{p}_i - \overline{\mathrm{c}}_{B_i})}_{\substack{= 0 \\ \text{since } \mathring{S}_i = \emptyset}}, \quad (36)$$
$$\leq -k \sum_{\substack{i \in \{1, \ldots, n\} \\ \mathring{S}_i \neq \emptyset}} m_{S_i} \|\mathrm{p}_i - \overline{\mathrm{c}}_{S_i}\|^2 \leq 0. \quad (37)$$

Hence, we have from Lasalle's Invariance Principle [23] that, at an equilibrium point of the "move-to-constrained-active-centroid" law, a robot is located at the constrained centroid, $\overline{\mathrm{c}}_{S_i}$, of its sensory cell, S_i, if it has a nonempty interior, i.e. $\mathring{S}_i \neq \emptyset$. Given that $\mathrm{p}_i = \overline{\mathrm{c}}_{S_i}$ for all $i \in \{1, \ldots, n\}$ with $\mathring{S}_i \neq \emptyset$, using (11), (33) and (34), one can further show that

$$\dot{\mathcal{H}}_{\mathcal{B}}\left(\mathbf{p}, \boldsymbol{\beta}+\boldsymbol{\epsilon}\right) = -k \sum_{\substack{i \in \{1, \ldots, n\} \\ \mathring{S}_i \neq \emptyset}} m_{B_i} \underbrace{2(\mathrm{p}_i - \mathrm{c}_{B_i})^{\mathrm{T}}(\mathrm{p}_i - \overline{\mathrm{c}}_{S_i})}_{\substack{= 0, \\ \text{since } \mathrm{p}_i = \overline{\mathrm{c}}_{S_i}}}$$
$$- k \sum_{\substack{i \in \{1, \ldots, n\} \\ \mathring{S}_i = \emptyset}} m_{B_i} \underbrace{2(\mathrm{p}_i - \mathrm{c}_{B_i})^{\mathrm{T}}(\mathrm{p}_i - \overline{\mathrm{c}}_{B_i})}_{\substack{\geq \|\mathrm{p}_i - \overline{\mathrm{c}}_{B_i}\|^2, \\ \text{since } \mathrm{p}_i \in F_i \text{ and } \|\mathrm{p}_i - \mathrm{c}_{B_i}\|^2 \geq \|\overline{\mathrm{c}}_{B_i} - \mathrm{c}_{B_i}\|^2}}, (38)$$
$$\leq -k \sum_{\substack{i \in \{1, \ldots, n\} \\ \mathring{S}_i = \emptyset}} m_{B_i} \|\mathrm{p}_i - \overline{\mathrm{c}}_{B_i}\|^2 \leq 0. \quad (39)$$

Therefore, at a stationary point of (33) ith robot is located at the constrained centroid, $\overline{\mathrm{c}}_{B_i}$, of its body cell B_i if $\mathring{S}_i = \emptyset$. Overall, by Lasalle's Invariance Principle, we have that any multirobot configuration starting in $\mathrm{Conf}\left(Q, \boldsymbol{\beta}+\boldsymbol{\epsilon}\right)$ asymptotically converges to a locally optimal sensing configuration in $G_{\mathcal{A}}\left(Q, \boldsymbol{\beta}+\boldsymbol{\epsilon}, \boldsymbol{\sigma}\right)$, which completes the proof. ∎

D. Coverage Control of Differential Drive Robots

Consider a noncolliding placement of a heterogeneous group of disk-shaped differential drive robots $(\mathbf{p}, \boldsymbol{\theta}) \in \mathrm{Conf}\left(Q, \boldsymbol{\beta}+\boldsymbol{\epsilon}\right) \times (-\pi, \pi]^n$ in a convex planar environment $Q \subset \mathbb{R}^2$ with associated vectors of body radii $\boldsymbol{\beta} \in \left(\mathbb{R}_{\geq 0}\right)^n$, safety margins $\boldsymbol{\epsilon} \in \left(\mathbb{R}_{>0}\right)^n$ and sensory footprint radii $\boldsymbol{\sigma} \in \left(\mathbb{R}_{\geq 0}\right)^n$, where $\boldsymbol{\theta} = \left(\theta_1, \theta_2, \ldots, \theta_n\right)$ is the vector of robot orientations.

The kinematic equations describing the motion of each differential drive robot are

$$\begin{aligned} \dot{\mathrm{p}}_i &= v_i \begin{bmatrix} \cos\theta_i \\ \sin\theta_i \end{bmatrix}, \\ \dot{\theta}_i &= \omega_i, \end{aligned} \quad (40)$$

where $v_i \in \mathbb{R}$ and $\omega_i \in \mathbb{R}$ are, respectively, the linear (tangential) and angular velocity inputs of ith robot. Note that the differential drive model is underactuated due to the nonholonomic constraint $\begin{bmatrix} -\sin\theta_i \\ \cos\theta_i \end{bmatrix}^{\mathrm{T}} \dot{\mathrm{p}}_i = 0$.

Let $\mathbb{S}\left(\mathbf{p}, \boldsymbol{\sigma}\right) = \{S_1, \ldots, S_n\}$ (9) be the sensory diagram of Q based on robot locations $\mathbf{p}$ and sensory footprint radii $\boldsymbol{\sigma}$, and $\mathcal{F}\left(\mathbf{p}, \boldsymbol{\beta}+\boldsymbol{\epsilon}\right) = \{F_1, \ldots, F_n\}$ (20) be the free subdiagram associated with configuration $\mathbf{p}$ and enlarged body radii $\boldsymbol{\beta}+\boldsymbol{\epsilon}$. For a choice of $\boldsymbol{\varepsilon} \in \left(\mathbb{R}_{>0}\right)^n$ with $\varepsilon_i > \epsilon_i$ for all i, we further define $\mathcal{T}\left(\mathbf{p}, \boldsymbol{\beta}+\boldsymbol{\varepsilon}\right) = \{T_1, T_2, \ldots, T_n\}$ to be

$$T_i := \mathrm{conv}\left(\{\mathrm{p}_i\} \cup F_i'\right) \quad (41)$$

where $\mathcal{F}\left(\mathbf{p}, \boldsymbol{\beta}+\boldsymbol{\varepsilon}\right) = \{F_1', F_2', \ldots, F_n'\}$ and $\mathrm{conv}\left(A\right)$ denotes the convex hull of set A. Note that, since $F_i' \subset F_i$, $\mathrm{p}_i \in F_i$ and F_i is convex, every element of $\mathcal{T}\left(\mathbf{p}, \boldsymbol{\beta}+\boldsymbol{\varepsilon}\right)$ is contained in the associated element of $\mathcal{F}\left(\mathbf{p}, \boldsymbol{\beta}+\boldsymbol{\epsilon}\right)$, i.e. $T_i \subseteq F_i$. It is useful to remark that we particularly require $\mathrm{p}_i \in T_i$ to guarantee an optimal choice of a local target

position in (45) relative to p_i, and we construct subset T_i of F_i to increase the convergence rate of our proposed coverage control law in (47).

As in the case of "move-to-constrained-centroid" law of fully actuated robots in (24), for optimal coverage each differential drive robot will intent to move towards the constrained centroid, $\overline{c}_{S_i}$ (23), of its sensory cell, S_i, but with a slight difference due to the nonholonomic constraint. To determine a linear velocity input guaranteeing collision avoidance, we select a safe target location that solves the following convex programming,

$$
\begin{aligned}
\text{minimize} \quad & \|q_i - c_{S_i}\|^2 \\
\text{subject to} \quad & q_i \in \overline{F}_i \cap H_i
\end{aligned} \tag{42}
$$

where

$$
H_i := \left\{ x \in Q \,\middle|\, \begin{bmatrix} \cos\theta_i \\ \sin\theta_i \end{bmatrix}^{\mathrm{T}} (x - p_i) = 0 \right\} \tag{43}
$$

is the straight line motion range due to the nonholonomic constraint. Note that $\overline{F}_i \cap H_i$ is a closed line segment in Q. Hence, once again, the unique solution of (42) is given by

$$
\overline{c}_{S_i}^{v} := \begin{cases} c_{S_i} & , \text{if } c_{S_i} \in \overline{F}_i \cap H_i, \\ \Pi_{\overline{F}_i \cap H_i}(c_{S_i}), & \text{otherwise,} \end{cases} \tag{44}
$$

where Π_C is the metric projection map onto a convex set C. Similarly, to determine robot's angular motion, we select another safe target location that solves

$$
\begin{aligned}
\text{minimize} \quad & \|q_i - c_{S_i}\|^2 \\
\text{subject to} \quad & q_i \in \overline{T}_i
\end{aligned} \tag{45}
$$

where $\overline{T}_i \subset \overline{F}_i$ is convex, and the unique solution of (45) is

$$
\overline{c}_{S_i}^{\omega} := \begin{cases} c_{S_i} & , \text{if } c_{S_i} \in \overline{T}_i, \\ \Pi_{\overline{T}_i}(c_{S_i}), & \text{otherwise.} \end{cases} \tag{46}
$$

Accordingly, based on a standard differential drive controller [25], we propose the following "move-to-constrained-centroid" law for differential drive robots,[15]

$$
v_i = -k \begin{bmatrix} \cos\theta_i \\ \sin\theta_i \end{bmatrix}^{\mathrm{T}} (p_i - \overline{c}_{S_i}^{v}), \tag{47a}
$$

$$
\omega_i = k \, \mathrm{atan} \left(\frac{\begin{bmatrix} -\sin\theta_i \\ \cos\theta_i \end{bmatrix}^{\mathrm{T}} (p_i - \overline{c}_{S_i}^{\omega})}{\begin{bmatrix} \cos\theta_i \\ \sin\theta_i \end{bmatrix}^{\mathrm{T}} (p_i - \overline{c}_{S_i}^{\omega})} \right), \tag{47b}
$$

where $k > 0$ is fixed. Having $G_{\mathcal{D}}(Q, \boldsymbol{\beta}, \boldsymbol{\epsilon}, \boldsymbol{\varepsilon}, \boldsymbol{\sigma})$ denote its set of stationary points where the constrained centroids $\overline{c}_{S_i}^{v}$ and $\overline{c}_{S_i}^{\omega}$ coincide and ith robot is located at $\overline{c}_{S_i}^{v} = \overline{c}_{S_i}^{\omega}$,

$$
G_{\mathcal{D}}(Q, \boldsymbol{\beta}, \boldsymbol{\epsilon}, \boldsymbol{\varepsilon}, \boldsymbol{\sigma}) := \left\{ p \in \mathrm{Conf}(Q, \boldsymbol{\beta}+\boldsymbol{\epsilon}) \,\middle|\, p_i = \overline{c}_{S_i}^{v} = \overline{c}_{S_i}^{\omega} \; \forall i \right\},
$$

we summarize important qualitative properties of the "move-to-constrained-centroid" law of differential drive robots as:

Proposition 4 *For any $\boldsymbol{\beta}, \boldsymbol{\sigma} \in (\mathbb{R}_{\geq 0})^n$ and $\boldsymbol{\epsilon}, \boldsymbol{\varepsilon} \in (\mathbb{R}_{>0})^n$ with $\epsilon_i < \varepsilon_i$ for all i, the "move-to-constrained-centroid" law of differential drive robots in (47) asymptotically steers all configurations in its positively invariant*

---

[15]To resolve indeterminacy we set $\omega_i = 0$ whenever $p_i = \overline{c}_{S_i}^{\omega}$.

---

domain $\mathrm{Conf}(Q, \boldsymbol{\beta}+\boldsymbol{\epsilon}) \times (-\pi, \pi]^n$ *towards the set of optimal sensing configurations* $G_{\mathcal{D}}(Q, \boldsymbol{\beta}, \boldsymbol{\epsilon}, \boldsymbol{\varepsilon}, \boldsymbol{\sigma}) \times (-\pi, \pi]^n$ *without increasing the utility function* $\mathcal{H}_{\mathcal{S}}(\cdot, \boldsymbol{\sigma})$ (10) *along the way.*

Proof. The configuration space $\mathrm{Conf}(Q, \boldsymbol{\beta}+\boldsymbol{\epsilon}) \times (-\pi, \pi]^n$ is positively invariant under the "move-to-constrained-centroid" law in (47) because, by construction (42), each robot's motion is constrained to the associated safe partition subcell in Q. The existence and uniqueness of its flow can be established using the pattern of the proof of Theorem 1 and the flow properties of the differential drive controller in [25].

Now, using $\mathcal{H}_{\mathcal{S}}(\cdot, \boldsymbol{\sigma})$ (10) as a continuously differentiable Lyapunov function, we obtain the stability properties as follows: for any $(\mathbf{p}, \boldsymbol{\theta}) \in \mathrm{Conf}(Q, \boldsymbol{\beta}+\boldsymbol{\epsilon}) \times (-\pi, \pi]^n$

$$
\dot{\mathcal{H}}_{\mathcal{S}}(\mathbf{p}, \boldsymbol{\sigma}) = -k \sum_{i=1}^{n} m_{S_i} \underbrace{2(p_i - c_{S_i})^{\mathrm{T}} (p_i - \overline{c}_{S_i}^{v})}_{\substack{\geq \|p_i - \overline{c}_{S_i}^{v}\|^2, \\ \text{since } p_i \in F_i \cap H_i \text{ and } \|p_i - c_{S_i}\|^2 \geq \|\overline{c}_{S_i}^{v} - c_{S_i}\|^2}}, \tag{48}
$$

$$
\leq -k \sum_{i=1}^{n} m_{S_i} \|p_i - \overline{c}_{S_i}^{v}\|^2 \leq 0, \tag{49}
$$

where $\dot{p}_i = -k(p_i - \overline{c}_{S_i}^{v})$. Hence, by LaSalle's Invariance Principle [23], at a stationary point of (47) ith robot is located at $\overline{c}_{S_i}^{v}$. Since for fixed $\overline{c}_{S_i}^{v}$ and $\overline{c}_{S_i}^{\omega}$ the standard differential drive controller asymptotically aligns each robot with the constrained centroid $\overline{c}_{S_i}^{\omega}$, i.e. $\begin{bmatrix} -\sin\theta_i \\ \cos\theta_i \end{bmatrix}^{\mathrm{T}} (p_i - \overline{c}_{S_i}^{\omega}) = 0$ [25], it is guaranteed by (42) and (45) that $\overline{c}_{S_i}^{v} = \overline{c}_{S_i}^{\omega}$ whenever $\|p_i - \overline{c}_{S_i}^{v}\| = 0$ and $\begin{bmatrix} -\sin\theta_i \\ \cos\theta_i \end{bmatrix}^{\mathrm{T}} (p_i - \overline{c}_{S_i}^{\omega}) = 0$. Therefore, we have from LaSalle's Invariance Principle that all configurations in $\mathrm{Conf}(Q, \boldsymbol{\beta}+\boldsymbol{\epsilon}) \times (-\pi, \pi]^n$ asymptotically reach $G_{\mathcal{D}}(Q, \boldsymbol{\beta}, \boldsymbol{\epsilon}, \boldsymbol{\varepsilon}, \boldsymbol{\sigma}) \times (-\pi, \pi]^n$. ∎

Finally, note that the "move-to-constrained-active-centroid" law of Section IV-C can be utilized for congestion control of differential drive robots by using active domains in (32) instead of the sensory diagram $\mathcal{S}(\mathbf{p}, \boldsymbol{\sigma})$, and the resulting coverage law maintains qualitative properties.

V. NUMERICAL SIMULATIONS

A common source of collisions between robots while performing a distributed sensing task is a concentrated event distribution which generally causes robots to move towards the same small region of the environment.[16] We therefore consider the following event distribution, $\phi : [0, 10]^2 \to \mathbb{R}_{>0}$, for a homogeneous group of disk-shaped robots operating in a 10×10 square environment,

$$
\phi(q) = e^{-\left\| q - \begin{bmatrix} 7 \\ 7 \end{bmatrix} \right\|^2}. \tag{50}
$$

In Fig. 3 we present the resulting trajectories of our proposed coverage control algorithms. Since the event distribution

---

[16]For all simulations we set $\epsilon_i = 0.05$ and $\varepsilon_i = 0.1$ for all $i \in \{1, 2, \ldots, n\}$, and all simulations are obtained through numerical integration of the associated coverage control law using the ode45 function of MATLAB, and the computation of the centroid of a power cell in (6) is approximated by discretizing the power cell by a 20×20 grid.
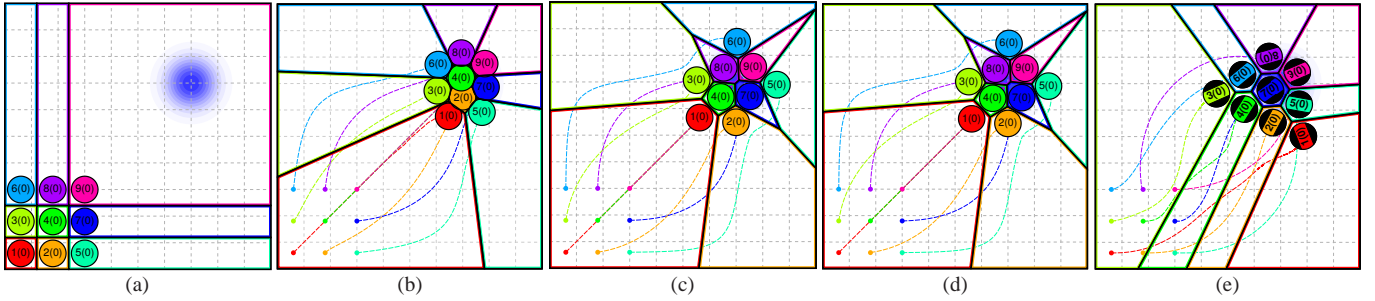
Fig. 3. Avoiding collisions around a concentrated event distribution. (a) Initial configuration of a homogeneous robot network, where the weight of sensory cell are shown in the parenthesis, and the resulting trajectories of (b) the standard "move-centroid" law (12), (c) the "move-to-constrained-centroid" law (24), (d) the "move-to-constrained-active-centroid" law (33), (e) the "move-to-constrained-centroid" law of differential drive robots (47) which are initially aligned with the horizontal axis.
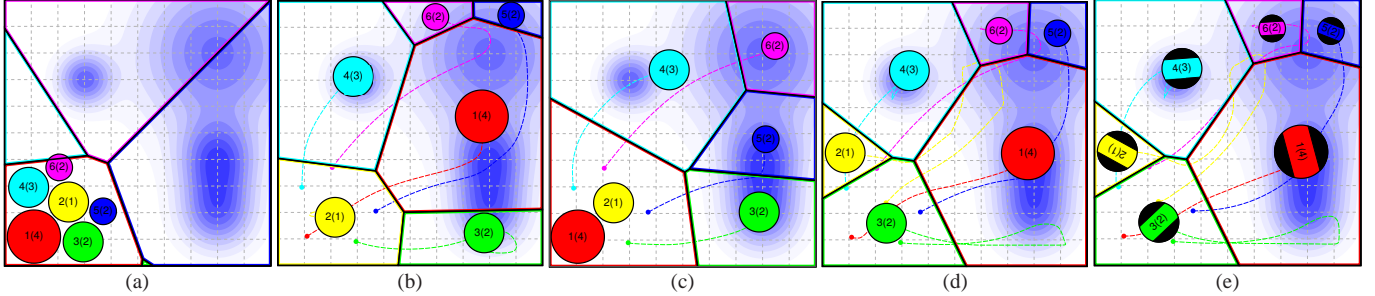

Fig. 4. Safe coverage control of heterogeneous disk-shaped robots with a heuristic management of unassigned robots. (a) Initial configuration of a heterogeneous robot network, where the weight of sensory cell are shown in the parenthesis, and the resulting trajectories of (b) the standard "move-centroid" law (12), (c) the "move-to-constrained-centroid" law (24), (d) the "move-to-constrained-active-centroid" law (33), (e) the "move-to-constrained-active-centroid" law of differential drive robots which are initially aligned with the horizontal axis.

is concentrated around a small region, as expected, the standard "move-to-centroid" law steers robots to a centroidal Voronoi configuration where robots collide. On the other hand, since a Voronoi partition has no occupancy defect, our "move-to-constrained-centroid" and "move-to-constrained-active-centroid" laws yield the same trajectory that asymptotically converges a collision free constrained centroidal Voronoi configuration. It is also well known that minimizing the location optimization function $\mathcal{H}_S$ (10) generally results in a locally optimal sensing configuration, and we observe in Figures 3.(c) and 3.(e) that, although they are initiated at the same location, fully actuated and differential drive robots asymptotically reach different constrained centroidal Voronoi configurations.

To demonstrate how unassigned robots may limit the mobility of others, we consider a heterogeneous group of disk-shaped robots operating in a 10×10 environment with the following event distribution function, $\phi : [0,10]^2 \rightarrow \mathbb{R}_{>0}$,

$$\phi(q) = 1 + 10e^{-\frac{1}{9}\left\|q - \left[\begin{smallmatrix} 8 \\ 8 \end{smallmatrix}\right]\right\|^2} + e^{-\frac{1}{2}\left\|q - \left[\begin{smallmatrix} 8 \\ 2 \end{smallmatrix}\right]\right\|^2} + e^{-\frac{1}{2}\left\|q - \left[\begin{smallmatrix} 8 \\ 4 \end{smallmatrix}\right]\right\|^2} + e^{-\left\|q - \left[\begin{smallmatrix} 3 \\ 7 \end{smallmatrix}\right]\right\|^2}, \quad (51)$$

which is also used in [7]. In Fig. 4 we illustrate the resulting trajectories of our safe coverage control algorithms. As seen in Fig. 4.(a), the 2nd robot is initially not assigned to any region. It stays stationary for a certain finite time under the the standard "move-to-centroid" law during which the 1st robot moves through it. Also notice that the 3rd robot violates the workspace boundary before converging a safe location. In summary, the "move-to-centroid" law steers disk-shaped

robots to a locally optimal sensing configuration without avoiding collisions along the way. Our "move-to-constrained-centroid" law prevents any possible self-collisions and collisions with the boundary of the environment. However, since the 2nd robot stays unassigned for all future time, the 1st robot is blocked and it can not move to a better coverage location. Fortunately, while guaranteeing collision avoidance, our "move-to-constrained-active-centroid" law steers unassigned robots to improve assigned robots' progress for both fully actuated and differential drive robots, as illustrated in Figures 4.(d) and 4.(e), respectively.

VI. CONCLUSION

In this paper we introduce a novel use of power diagrams for identifying collision free multirobot configurations, and propose a constrained optimization framework combining coverage control and collision avoidance for fully actuated disk-shaped robots, comprising the main contributions of the paper. We also present its extensions for the widely used differential drive model and for congestion management of unassigned robots. Numerical simulations demonstrate the effectiveness of the proposed coverage control algorithms.

Work now in progress targets another extension of Voronoi-based coverage control for hierarchical settings, based on nested partitions of convex environments [26].We also believe that encoding collision free configurations in terms of power diagrams might have a significant value for robot motion planning, and we are currently exploring its possible usage in the design of feedback motion planners.

REFERENCES

[1] M. Schwager, D. Rus, and J.-J. Slotine, "Unifying geometric, probabilistic, and potential field approaches to multi-robot deployment," *Int. J. Robotics Research*, vol. 30, no. 3, pp. 371–383, 2011.

[2] J. Cortés, S. Martınez, T. Karatas, and F. Bullo, "Coverage control for mobile sensing networks," *Robotics and Automation, IEEE Transactions on*, vol. 20, no. 2, pp. 243–255, 2004.

[3] A. Okabe, B. Boots, K. Sugihara, and S. N. Chiu, *Spatial tessellations: concepts and applications of Voronoi diagrams*, 2nd ed. John Wiley & Sons, 2000, vol. 501.

[4] L. Pimenta, V. Kumar, R. Mesquita, and G. Pereira, "Sensing and coverage for a network of heterogeneous robots," in *Decision and Control (CDC), IEEE Conference on*, 2008, pp. 3947–3952.

[5] Y. Kantaros, M. Thanou, and A. Tzes, "Distributed coverage control for concave areas by a heterogeneous robotswarm with visibility sensing constraints," *Automatica*, vol. 53, pp. 195 – 207, 2015.

[6] A. Pierson, L. C. Figueiredo, L. C. A. Pimenta, and M. Schwager, "Adapting to performance variations in multi-robot coverage," in *Robotics and Automation (ICRA), IEEE Int. Conference on*, 2015.

[7] A. Kwok and S. Martnez, "Deployment algorithms for a power-constrained mobile sensor network," *International Journal of Robust and Nonlinear Control*, vol. 20, no. 7, pp. 745–763, 2010.

[8] F. Aurenhammer, "Power diagrams: Properties, algorithms and applications," *SIAM Journal on Computing*, vol. 16, no. 1, pp. 78–96, 1987.

[9] A. Dirafzoon, M. Menhaj, and A. Afshar, "Voronoi based coverage control for nonholonomic mobile robots with collision avoidance," in *Control Applications (CCA), IEEE Int. Conf. on*, 2010, pp. 1755–1760.

[10] L. Pimenta, M. Schwager, Q. Lindsey, V. Kumar, D. Rus, R. Mesquita, and G. Pereira, "Simultaneous coverage and tracking (scat) of moving targets with robot networks," in *Algorithmic Foundation of Robotics VIII*, ser. Springer Advanced Robotics, 2010, vol. 57, pp. 85–99.

[11] A. Breitenmoser and A. Martinoli, "On combining multi-robot coverage and reciprocal collision avoidance," in *Procedings of the Twelfth Int. Symp. on Distributed Autonomous Robotic Systems*, 2014.

[12] Y. Kantaros, M. Thanou, and A. Tzes, "Visibility-oriented coverage control of mobile robotic networks on non-convex regions," in *Robotics and Automation, IEEE Int. Conf. on*, 2014, pp. 1126–1131.

[13] H. W. Hamacher and Z. Drezner, *Facility location: applications and theory*. Springer Science & Business Media, 2002.

[14] S. Lloyd, "Least squares quantization in pcm," *Information Theory, IEEE Transactions on*, vol. 28, no. 2, pp. 129–137, 1982.

[15] Q. Du, V. Faber, and M. Gunzburger, "Centroidal voronoi tessellations: Applications and algorithms," *SIAM Review*, vol. 41, no. 4, pp. 637–676, 1999.

[16] F. Bullo, J. Cortés, and S. Martinez, *Distributed Control of Robotic Networks: A Mathematical Approach to Motion Coordination Algorithms*. Princeton University Press, 2009.

[17] R. Haralick, S. R. Sternberg, and X. Zhuang, "Image analysis using mathematical morphology," *Pattern Analysis and Machine Intelligence, IEEE Transactions on*, vol. 9, no. 4, pp. 532–550, 1987.

[18] S. Boyd and L. Vandenberghe, *Convex Optimization*. Cambridge University Press, 2004.

[19] M. Kozlov, S. Tarasov, and L. Khachiyan, "The polynomial solvability of convex quadratic programming," {*USSR*} *Computational Mathematics and Mathematical Physics*, vol. 20, no. 5, pp. 223 – 228, 1980.

[20] L. Kuntz and S. Scholtes, "Structural analysis of nonsmooth mappings, inverse functions, and metric projections," *Journal of Mathematical Analysis and Applications*, vol. 188, no. 2, pp. 346 – 386, 1994.

[21] Q. Du, M. D. Gunzburger, and L. Ju, "Constrained centroidal voronoi tessellations for surfaces," *SIAM Journal on Scientific Computing*, vol. 24, no. 5, pp. 1488–1506, 2003.

[22] R. W. Chaney, "Piecewise ck functions in nonsmooth analysis," *Nonlinear Analysis: Theory, Methods & Applications*, vol. 15, no. 7, pp. 649 – 660, 1990.

[23] H. K. Khalil, *Nonlinear Systems*, 3rd ed. Prentice Hall, 2001.

[24] M. W. Hirsch, S. Smale, and R. L. Devaney, *Differential equations, dynamical systems, and an introduction to chaos*, 2nd ed. Academic press, 2003.

[25] A. Astolfi, "Exponential stabilization of a wheeled mobile robot via discontinuous control," *Journal of dynamic systems, measurement, and control*, vol. 121, no. 1, pp. 121–126, 1999.

[26] O. Arslan, D. Guralnik, and D. E. Koditschek, "Navigation of distinct euclidean particles via hierarchical clustering," in *Algorithmic Foundations of Robotics XI*, ser. Springer Tracts in Advanced Robotics, 2015, vol. 107, pp. 19–36.